

A Local Discontinuous Galerkin Method for Dirichlet Boundary Control Problems

Peter Benner* Michael Hinze†
 Hamdullah Yücel ‡

Dedicated to our long-standing, highly esteemed colleague and friend Ronald Hoppe

January 28, 2026

Abstract

In this paper, we consider control constrained L^2 –Dirichlet boundary control of a convection-diffusion equation on a two dimensional convex polygonal domain. We discretize the control problem based on the local discontinuous Galerkin method with piecewise linear ansatz functions for the flux and potential. We derive a priori error estimates for the full as well as for the variational discrete control approximation. We present a selection of numerical results to demonstrate the performance of our approach and to underpin the theoretical findings.

1 Introduction

Let $\Omega \subset \mathbb{R}^2$ be a bounded, convex open domain with a Lipschitz boundary Γ . In the present work we are interested in the numerical analysis of the Dirichlet boundary control problem

$$\underset{u \in U^{\text{ad}}}{\text{minimize}} \quad \frac{1}{2} \|y - y^d\|_{0,\Omega}^2 + \frac{\omega}{2} \|u\|_{0,\Gamma}^2 =: J(y, u) \quad (1)$$

subject to

$$\begin{aligned} \nabla \cdot (-\epsilon \nabla y + \beta y) + \alpha y &= f && \text{in } \Omega, \\ y &= u && \text{on } \Gamma, \end{aligned} \quad (2)$$

where the admissible control set U^{ad} is specified by

$$U^{\text{ad}} := \{u \in L^2(\Gamma) : u^a \leq u(x) \leq u^b \text{ a.e. } x \in \Gamma\}, \quad (3)$$

with the real numbers u_a and u_b satisfying $u_a \leq u_b$. For the discretization of this control problem we consider variational discretization [31] and a P_1 discontinuous Galerkin approximation of the control variable. In both cases we employ the local discontinuous Galerkin (LDG) method for the discretization of the state.

*Max Planck Institute for Dynamics of Complex Technical Systems, Magdeburg, Germany, benner@mpi-magdeburg.mpg.de

†Mathematisches Institut, Universität Koblenz-Landau, Koblenz, Germany, hinze@uni-koblenz.de

‡Institute of Applied Mathematics, Middle East Technical University, Ankara, Türkiye, yucelh@metu.edu.tr

Contribution: For both control schemes we present a general estimate for the control and state errors. For the variational discrete scheme we in Theorem 4.1 for $u \in H^s(\Gamma)$ ($s \in [0, 1]$) obtain the error relation

$$\|u - u_h\|_{0,\Gamma} + \|y - y_h\|_{0,\Omega} \sim \|y - y_h(u)\|_{0,\Omega} + \|(\mathbf{p}_h(u) - \mathbf{p}) \cdot \mathbf{n}\|_{0,\Gamma} + \|z_h(u) - z\|_{0,\Gamma} =: E(y, \mathbf{p}, z),$$

which only includes Galerkin approximation errors for the primal potential y , as well as for the adjoint flux \mathbf{p} and the adjoint potential z . For the fully discrete case we in Theorem 4.2 obtain the error relation

$$\begin{aligned} \|u - u_h\|_{0,\Gamma} + \|y - y_h\|_{0,\Omega} &\sim E(y, \mathbf{p}, z) + \\ &+ \|\pi_h u - u\|_{0,\Gamma} + ((\mathbf{p}_h - \mathbf{p}(y_h)) \cdot \mathbf{n})_{0,\Gamma} + \|z_h - z(y_h)\|_{0,\Gamma} \end{aligned}$$

$^{1/2} \|\pi_h u - u\|_{0,\Gamma}^{1/2} + \|\pi_h u - u\|_{-s,\Gamma}^{1/2}$, which in addition to the Galerkin approximation errors for y, z , and \mathbf{p} also contains approximation errors for the auxiliary adjoint flux $\mathbf{p}(y_h)$ and potential $z(y_h)$, as well as projection errors associated with the Carstensen quasi-interpolation operator π_h . We would like to emphasize that our numerical analysis is inspired by the techniques introduced in [34, Chapter 3] and does not rely on the stability and continuity properties of the discrete solution operator associated with the LDG approximation scheme, thus differing from common practices in the literature, compare, e.g. [30, 45]. In the fully discrete case we for the error estimation only rely on the uniform boundedness of the discrete optimal states y_h in the $L^2(\Omega)$ norm, which one easily deduces from the structure of the cost functional together with the boundedness of the continuous solution operator. For our LDG approach with P_1 elements to approximate the discrete fluxes and potentials we obtain

$$\|u - u_h\|_{0,\Gamma} + \|y - y_h\|_{0,\Omega} \sim h^{1/2}$$

for both, the fully discrete and the variational discrete approaches. This is in accordance with the results reported in [27] for the case $k = 0$, i.e., where piecewise constant fluxes, piecewise linear potentials, and piecewise linear controls for the approximation of the control problem are utilized and convergence with $h^{1/2}$ is shown, no matter how smooth the involved states and potentials are. One conclusion from the analysis here can be that in the context of DG methods stability only comes at the expense of accuracy.

Finite element approximation of optimal control problems has been an active research area in engineering design for a long time, and has been extensively studied for many scientific and engineering applications. We refer to the monographs [34, 46, 48], as well as the references therein for the theory of the optimal control problems and for the development of numerical methods. Compared to distributed control problems, in which the control acts throughout the domain Ω , there has been relatively less research on boundary control problems. Moreover, the majority of existing studies on the boundary control problems focus on Neumann boundary control problems (see, e.g. [4, 11, 26, 33]), where the control is applied through Neumann boundary conditions rather than through conditions of the form (2). In contrast to distributed and Neumann control problems, Dirichlet boundary control poses additional challenges in both theoretical and numerical analysis, as the Dirichlet boundary data cannot be directly incorporated into a standard variational formulation. As a result, various alternative formulations have been proposed by researchers.

The first approach involves approximating the nonhomogeneous Dirichlet boundary condition using a Robin boundary condition or a weak boundary penalization method; see, e.g., [5, 6]. The second one, which is adopted in the present study, employs the $L^2(\Gamma)$ norm. In this case, the traditional finite element method treats the state variable in a very weak sense, as the nonhomogeneous Dirichlet boundary condition is prescribed only in $L^2(\Gamma)$. Extensive numerical studies have been conducted on elliptic Dirichlet boundary control problems using this formulation. We refer to [3, 13, 23, 43, 42, 45] for a priori error estimates, and to [2] for the regularity analysis. In [13], a control-constrained optimal control problem governed by a semilinear elliptic equation in a convex polygonal domain was investigated, where error estimates of order h^s for both the

control and state variables were derived with $s < \min(1, \pi/(2\theta))$ and θ denoting the largest interior angle of the domain. Subsequently, an enhanced error estimate of order $h^{3/2}$ for the control variable in the case of smooth domains was presented in [23] by exploiting the superconvergence properties of regular triangulations. Then, improved convergence rates for the state variable in the unconstrained case on convex domains were obtained in [43] through a duality argument combined with a control estimate in a norm weaker than $L^2(\Gamma)$. Later, error estimates of order h^s , with $s < \min(1, \pi/\theta - 1/2)$ for general meshes and $s < \min(3/2, \pi/\theta - 1/2)$ for superconvergent meshes, were established for the control variable on general polygonal domains in [3]. Another common approach to formulate Dirichlet boundary control problem is the energy space method, where the L^2 -norm in the cost functional is replaced with $H^{1/2}$ -norm. This choice of control space allows for a standard weak formulation of the state equation and produces optimal estimates on a convex polygonal domain; however, it introduces an additional operator, the Steklov–Poincaré operator, through the harmonic extension of the given Dirichlet boundary data; see, e.g., [44, 49]. In a similar fashion, the H^1 -norm, which naturally results in harmonic control, is utilized in [18, 38] to regularize the control variable. Further, it is noted in [24] that a fourth-order formulation of the adjoint variable, derived by eliminating the control and state variables, is employed to address Dirichlet boundary control problems.

Unlike continuous finite element approximations of the state variables, alternative discretization techniques, such as the mixed finite element method [30] and the hybridizable discontinuous Galerkin (HDG) [36] method, have been employed to overcome the challenges arising from the variational formulation of continuous finite element methods. In [30], the error estimates of order $h^{1-1/s}$ with $s \geq 2$ were established polygonal domains and of order $h|\ln h|$ for smooth domains, where the classical RT_0 mixed finite element method was used for the approximation. In [36] a HDG method with discrete fluxes in P_k and potentials in P_{k+1} for $k \geq 0$ was applied. Error estimates of order h^s for $s < \min(3/2, \pi/\theta - 1/2)$ for $k \geq 1$, and of order $h^{1/2}$ in the case $k = 0$ were reported.

All of the aforementioned studies concentrate on Dirichlet boundary control for elliptic equations. However, such control problems are also of significant importance in various applications governed by fluid dynamics models, including the Stokes [28, 29] and Navier–Stokes equations [25, 32]. Prior to analyzing the numerical behavior of complex optimal control problems governed by fluid dynamics models, it is essential to first study optimization problems constrained by convection–diffusion equations. Numerical studies for unconstrained Dirichlet boundary control problems governed by a convection–diffusion equation have been carried out in [27, 35, 16] using a HDG method, and in [22] employing a symmetric interior penalty Galerkin approach. In the present work we focus on the numerical analysis of Dirichlet boundary control problems governed by a convection–diffusion equation with L^2 –boundary controls subject to pointwise bounds on the control. The local discontinuous Galerkin (LDG) method is employed as a discretization technique to address the variational challenges that arise when the control space is taken as $L^2(\Gamma)$ and to leverage the strengths of discontinuous Galerkin methods for convection–diffusion equations. The LDG method is one of several discontinuous Galerkin approaches that have been extensively studied, particularly for convection–diffusion problems, due to their versatility in handling a wide range of applications and their advantageous features such as local conservativity and strong locality. It uses P_k ($k \geq 1$) elements for the approximation of discrete fluxes and potentials. For studies on the use of discontinuous Galerkin methods in convection-dominated PDEs, we refer the reader to [9, 15, 47, 17, 20]. In the present work we use the results from [14, 19, 37] to estimate the approximation errors of the states and adjoint states. Finally, let us mention that optimal control problems governed by convection–diffusion equations were investigated in [7, 40, 50, 51, 52].

The rest of this paper is organized as follows: In the following section we discuss the regularity of the solutions under the appropriate assumptions and notation and present the optimality system. Section 3 is devoted to the formulation of the LDG scheme for approximating the Dirichlet boundary control problem. In Section 4, we establish a priori error estimates for the LDG approximation on a convex polygonal domain. These estimates are derived for two distinct discretization strategies used in the optimal control problem: the variational discretization approach and the piecewise linear discretization approach. Section 5 provides numerical experiments to support and

validate the theoretical findings. Finally, concluding remarks and further discussion are presented in Section 6.

2 Regularity and optimality system

Throughout this paper we adopt the standard notation $W^{m,p}(\Omega)$ (see, e.g., [1]) for Sobolev spaces equipped with the norm $\|\cdot\|_{m,p,\Omega}$ and seminorm $|\cdot|_{m,p,\Omega}$ for $m \geq 0$ and $1 \leq p \leq \infty$ on an open bounded domain Ω in \mathbb{R}^2 with the boundary $\Gamma = \partial\Omega$. We denote $W^{m,2}(\Omega)$ by $H^m(\Omega)$ with norm $\|\cdot\|_{m,\Omega}$ and seminorm $|\cdot|_{m,\Omega}$. The space of square integrable functions over Ω is represented by $L^2(\Omega)$, with the norm $\|\cdot\|_{0,\Omega}$ and the inner products on $L^2(\Omega)$ and $L^2(\Gamma)$ are defined by

$$(v, w)_\Omega = \int_\Omega v w \, dx \quad \forall v, w \in L^2(\Omega), \quad \text{and} \quad \langle v, w \rangle_\Gamma = \int_\Gamma v w \, ds \quad \forall v, w \in L^2(\Gamma),$$

respectively. Note that $H_0^1 = \{v \in H^1(\Omega) : v = 0 \text{ on } \partial\Omega\}$. Moreover, C denotes a generic positive constant independent of the mesh size h and may differ in various estimates. For clarity and convenience, we assume the following conditions on the domain Ω and the given data, which are valid throughout the paper:

Assumption 2.1. *We assume that Ω is a convex polygonal domain in \mathbb{R}^2 with Lipschitz boundary Γ and $\theta \in [\pi/3, \pi)$ represents the largest interior angle of Ω . Diffusion and regularization parameters denoted by ϵ and ω are positive constants. The velocity field $\beta \in (W^{1,\infty}(\Omega))^2$ complies with incompressibility condition, that is, $\nabla \cdot \beta = 0$. The reaction function $\alpha \in L^\infty(\Omega)$ satisfies $\alpha(x) \geq 0$. For the source function f and the desired state y^d , we assume $f, y^d \in L^2(\Omega)$.*

Owing to the low a priori regularity of the control $u \in U := L^2(\Gamma)$ in the optimal control problem (1), the state equation (2) is understood in a very weak sense, i.e., we seek a solution $y \in L^2(\Omega)$ satisfying

$$-\epsilon(y, \Delta v)_\Omega - (y, \beta \cdot \nabla v)_\Omega + (\alpha y, v)_\Omega = (f, v)_\Omega - \epsilon \langle u, \partial_n v \rangle_\Gamma \quad (4)$$

for all $v \in H_0^1(\Omega) \cap H^2(\Omega)$ with $\partial_n v := \nabla v \cdot \mathbf{n}$ and \mathbf{n} representing the unit outward normal vector to Γ . It is well known that problem (4) for $f \in L^2(\Omega)$ and $u \in L^2(\Gamma)$ admits a unique solution $y \in H^{1/2}(\Omega)$, which satisfies

$$\|y\|_{H^{1/2}(\Omega)} \leq C(\|f\|_{0,\Omega} + \|u\|_{0,\Gamma}), \quad (5)$$

compare, e.g. [12, 39, 45].

Based on the very weak formulation of the state equation (4), the optimal control problem (1)-(2) can be stated as follows

$$\underset{(y,u) \in L^2(\Omega) \times U^{\text{ad}}}{\text{minimize}} \quad J(y, u) \text{ subject to (4).} \quad (6)$$

Using the standard arguments in the present setting, it can be shown that problem (6) admits a unique solution $(y, u) \in H^1(\Omega) \times (H^{1/2}(\Gamma) \cap U^{\text{ad}})$, which together with the unique adjoint state $z \in H^2(\Omega) \cap H_0^1(\Omega)$ weakly solves the following optimality system

$$\begin{aligned} \nabla \cdot (-\epsilon \nabla y + \beta y) + \alpha y &= f && \text{in } \Omega, \\ y &= u && \text{on } \Gamma, \end{aligned} \quad (7a)$$

$$\begin{aligned} \nabla \cdot (-\epsilon \nabla z - \beta z) + \alpha z &= y - y^d && \text{in } \Omega, \\ z &= 0 && \text{on } \Gamma, \end{aligned} \quad (7b)$$

and

$$\langle \omega u - \epsilon \partial_n z, w - u \rangle_\Gamma \geq 0 \quad w \in U^{\text{ad}}. \quad (7c)$$

Since $z \in H^2(\Omega) \cap H_0^1(\Omega)$, it follows for convex polyhedral domains from, e.g., [45, Th. 2.5] that $\partial_n z \in H^{1/2}(\Gamma)$. The variational inequality (7c) is equivalent to $u = \mathcal{P}_{U^{\text{ad}}}(\frac{\epsilon}{\omega} \partial_n z) \in H^{1/2}(\Gamma)$, compare, e.g. [39, Lemma 3.3]. Here, $\mathcal{P}_{U^{\text{ad}}}$ denotes the orthogonal projection in $L^2(\Gamma)$ onto the admissible set U^{ad} . Since (7a) for every $u \in U^{\text{ad}}$ admits a unique very weak solution $y(u)$, the reduced cost functional $\widehat{J}(u) := J(y(u), u)$ is well-defined. Furthermore, $\widehat{J}'(u) = \omega u - \epsilon \partial_n z$, where z denotes the unique adjoint state satisfying (7b) with $y = y(u)$.

To apply the local discontinuous Galerkin (LDG) method for approximating the solution of the Dirichlet boundary control problem (1)–(2), we employ a mixed formulation of the optimality system (7a)–(7c). This is possible since the optimal control of problem (6) satisfies $u \in H^{1/2}(\Gamma)$ and in this case it follows from (4) that $\nabla y \in H(\text{div}, \Omega)$ holds, so that $\nabla y \cdot \mathbf{n} \in H^{-1/2}(\Gamma)$, compare [36, 30]. One now has that with the unique solution (y, z, u) of the optimality system (7a)–(7c) the functions $y, \mathbf{q}, z, \mathbf{p}, u$ with $\mathbf{q} := -\epsilon^{\frac{1}{2}} \nabla y$, $\mathbf{p} := \epsilon^{\frac{1}{2}} \nabla z$, $\mathbf{q}, \mathbf{p} \in H(\text{div}, \Omega)$, form the unique weak solution of the mixed system given by

$$\begin{aligned} \nabla \cdot (\beta y + \epsilon^{\frac{1}{2}} \mathbf{q}) + \alpha y &= f && \text{in } \Omega, \\ \mathbf{q} &= -\epsilon^{\frac{1}{2}} \nabla y && \text{in } \Omega, \\ y &= u && \text{on } \Gamma. \end{aligned} \tag{8a}$$

$$\begin{aligned} \nabla \cdot (-\beta z - \epsilon^{\frac{1}{2}} \mathbf{p}) + \alpha z &= y - y^d && \text{in } \Omega, \\ \mathbf{p} &= \epsilon^{\frac{1}{2}} \nabla z && \text{in } \Omega, \\ z &= 0 && \text{on } \Gamma. \end{aligned} \tag{8b}$$

$$\langle \omega u - \epsilon^{\frac{1}{2}} \mathbf{p} \cdot \mathbf{n}, w - u \rangle_{\Gamma} \geq 0, \quad \forall w \in U^{\text{ad}}. \tag{8c}$$

To ensure the approximation properties of the LDG method, specific regularity assumptions on the involved states and fluxes are required. For the solution of our optimal Dirichlet boundary control problem in polygonal domains a detailed study can be found in [2]. We in this respect from e.g. [35, Theorem 2.10] have the following theorem, which is also valid in our control constrained case, compare the investigations in [2, Section 4] related to the convex case.

Theorem 2.2. *Suppose that Assumption 2.1 is satisfied and $y^d \in H^t(\Omega)$ with $0 \leq t < 1$. Then, for $s \in [\frac{1}{2}, \min\{\frac{1}{2} + t, \pi/\theta - 1/2\}]$ we for the solution of the optimality system (8a)–(8c) have*

$$u \in H^s(\Gamma), \quad y \in H^{s+1/2}(\Omega), \quad \mathbf{q} \in H^{s-1/2}(\Omega)^2 \cap H(\text{div}, \Omega),$$

as well as

$$z \in H^{s+3/2}(\Omega) \cap H_0^1(\Omega) \quad \text{and} \quad \mathbf{p} \in H^{s+1/2}(\Omega)^2 \cap H(\text{div}, \Omega).$$

3 Local discontinuous Galerkin formulation

Since we assume that the domain Ω is polygonal, its boundary is exactly represented by triangle edges. We denote $\{\mathcal{T}_h\}_h$ as a family of shape-regular simplicial triangulations of Ω . Each mesh \mathcal{T}_h consists of closed triangles such that $\Omega = \bigcup_{K \in \mathcal{T}_h} K$ holds. We assume that the mesh is regular in the following sense: for different triangles $K_i, K_j \in \mathcal{T}_h$, $i \neq j$, the intersection $K_i \cap K_j$ is either empty or a vertex or an edge, i.e., hanging nodes are not allowed. The diameter of an element K and the length of an edge E are denoted by h_K and h_E , respectively, with $h = \max_{K \in \mathcal{T}_h} h_K$. The set of all edges \mathcal{E}_h is split into the set \mathcal{E}_h^0 of interior edges and the set \mathcal{E}_h^{∂} of boundary edges so that

$\mathcal{E}_h = \mathcal{E}_h^0 \cup \mathcal{E}_h^\partial$. For the outward normal unit vector \mathbf{n} on Γ , the inflow and outflow parts of Γ are denoted by Γ^- and Γ^+ , respectively,

$$\Gamma^- = \{x \in \Gamma : \beta \cdot \mathbf{n} < 0\}, \quad \Gamma^+ = \{x \in \Gamma : \beta \cdot \mathbf{n} \geq 0\}.$$

Similarly, the boundaries of an element $K \in \mathcal{T}_h$ can be categorized into inflow and outflow boundaries: ∂K^- and ∂K^+ .

Let the edge E be a common edge for two elements K and K^e . For a piecewise continuous scalar function y , there are two traces of y along E , denoted by $y|_E$ from inside K and $y^e|_E$ from inside K^e . Then, the jump and average of y across the edge E are defined by:

$$[\![y]\!] = y|_E \mathbf{n}_K + y^e|_E \mathbf{n}_{K^e}, \quad \{\{y\}\} = \frac{1}{2}(y|_E + y^e|_E),$$

where \mathbf{n}_K (resp. \mathbf{n}_{K^e}) denotes the unit outward normal to ∂K (resp. ∂K^e). Similarly, for a piecewise continuous vector field \mathbf{q} , the jump and average across an edge E are given, respectively, by

$$[\![\mathbf{q}]\!] = \mathbf{q}|_E \cdot \mathbf{n}_K + \mathbf{q}^e|_E \cdot \mathbf{n}_{K^e}, \quad \{\{\mathbf{q}\}\} = \frac{1}{2}(\mathbf{q}|_E + \mathbf{q}^e|_E).$$

For a boundary edge $E \in K \cap \Gamma$, we set $\{\{\mathbf{q}\}\} = \mathbf{q}$ and $[\![y]\!] = y\mathbf{n}$, where \mathbf{n} is the outward normal unit vector on Γ . Note that the jump in y is a vector and the jump in \mathbf{q} is a scalar which only involves the normal component of \mathbf{q} .

To adapt the continuous mixed solution setting to the LDG solution setting we note that the weak solution of (8a) also satisfies the following elementwise system on an element $K \in \mathcal{T}_h$

$$-(\epsilon^{\frac{1}{2}} \mathbf{q} + \beta y, \nabla v)_K + (\alpha y, v)_K + \langle (\epsilon^{\frac{1}{2}} \mathbf{q} + \beta y) \cdot \mathbf{n}, v \rangle_{\partial K} = (f, v)_K \quad v \in V, \quad (9a)$$

$$(\mathbf{q}, \mathbf{r})_K - (\epsilon^{\frac{1}{2}} y, \nabla \cdot \mathbf{r})_K + \langle \epsilon^{\frac{1}{2}} u, \mathbf{r} \cdot \mathbf{n} \rangle_{\partial K} = 0 \quad \mathbf{r} \in \mathbf{W}, \quad (9b)$$

where

$$\begin{aligned} \mathbf{W} &:= \left\{ \mathbf{w} \in (L^2(\Omega))^2 : \mathbf{w}_K \in (H^1(K))^2, \forall K \in \mathcal{T}_h \right\}, \\ V &:= \left\{ v \in L^2(\Omega) : v_K \in H^1(K), \forall K \in \mathcal{T}_h \right\}. \end{aligned}$$

Next, we seek to approximate the state solution (y, \mathbf{q}) with functions (y_h, \mathbf{q}_h) in the following finite element spaces $\mathbf{W}_h \times V_h \subset \mathbf{W} \times V$:

$$\mathbf{W}_h = \left\{ \mathbf{w} \in (L^2(\Omega))^2 : \mathbf{w}|_K \in (\mathbb{S}^1(K))^2, \forall K \in \mathcal{T}_h \right\}, \quad (10a)$$

$$V_h = \left\{ v \in L^2(\Omega) : v|_K \in \mathbb{S}^1(K), \forall K \in \mathcal{T}_h \right\}, \quad (10b)$$

$$U_h = \left\{ u \in L^2(\Gamma) : u|_E \in \mathbb{S}^1(E), \forall E \in \mathcal{E}_h^\partial \right\}, \quad (10c)$$

where $\mathbb{S}^1(K)$ (resp. $\mathbb{S}^1(E)$) is the local finite element space, which consists of linear polynomials in each element K (resp. on E). Then, for all $(v, \mathbf{r}) \in (V_h \times \mathbf{W}_h)$ the approximate solution (y_h, \mathbf{q}_h) of the state solution (y, \mathbf{q}) satisfies

$$-(\epsilon^{\frac{1}{2}} \mathbf{q}_h + \beta y_h, \nabla v)_K + (\alpha y_h, v)_K + \langle (\epsilon^{\frac{1}{2}} \widehat{\mathbf{q}}_h + \beta \widehat{y}_h) \cdot \mathbf{n}, v \rangle_{\partial K} = (f, v)_K, \quad (11a)$$

$$(\mathbf{q}_h, \mathbf{r})_K - (\epsilon^{\frac{1}{2}} y_h, \nabla \cdot \mathbf{r})_K + \langle \epsilon^{\frac{1}{2}} \widehat{y}_h, \mathbf{r} \cdot \mathbf{n} \rangle_{\partial K} = 0. \quad (11b)$$

The numerical fluxes, denoted as $\widehat{\mathbf{q}}_h$, \widehat{y}_h , and \widehat{y}_h , must be appropriately defined to ensure the stability of the method and to improve its accuracy.

We are now ready to introduce the expressions that define the numerical fluxes. The numerical traces of y_h associated with the diffusion and convection terms are characterized, respectively, as

$$\widehat{y}_h = \begin{cases} \{\{y_h\}\} + \mathbf{C}_{12} \cdot [\![y_h]\!], & E \in \mathcal{E}_h^0, \\ u_h, & E \in \mathcal{E}_h^\partial, \end{cases} \quad \text{and} \quad \widetilde{y}_h = \begin{cases} u_h, & E \in \Gamma^-, \\ \{\{y_h\}\} + \mathbf{D}_{11} \cdot [\![y_h]\!], & E \in \mathcal{E}_h^0, \\ y_h, & E \in \Gamma^+. \end{cases} \quad (12)$$

From (12), it is seen that the numerical trace \tilde{y}_h aligns with the traditional upwinding trace. Moreover, the numerical flux $\hat{\mathbf{q}}_h$ is given by

$$\hat{\mathbf{q}}_h = \begin{cases} \{\mathbf{q}_h\} - C_{11}[\![y_h]\!] - \mathbf{C}_{12}[\![\mathbf{q}_h]\!], & E \in \mathcal{E}_h^0, \\ \mathbf{q}_h - C_{11}(y_h - u_h) \cdot \mathbf{n}, & E \in \mathcal{E}_h^\partial. \end{cases} \quad (13)$$

Here, we set $C_{11} = \epsilon/h_E$ for each $E \in \mathcal{E}_h$, choose \mathbf{C}_{12} as $\mathbf{C}_{12} \cdot \mathbf{n} = \frac{1}{2} \text{sign}(\mathbf{n} \cdot \mathbf{v})$ for a nonzero arbitrary vector \mathbf{v} , and define the vector-valued function \mathbf{D}_{11} as follows

$$\mathbf{D}_{11} \cdot \mathbf{n} = \frac{1}{2} \text{sign}(\mathbf{n} \cdot \beta).$$

For a more detailed discussion, we refer to [14, 19, 21, 52].

Putting the numerical fluxes in (12)-(13) into (11) and summing over all elements, we obtain

$$\begin{aligned} & - \sum_{K \in \mathcal{T}_h} \int_K (\epsilon^{\frac{1}{2}} \mathbf{q}_h + \beta y_h) \cdot \nabla v \, dx + \sum_{E \in \mathcal{E}_h^0} \int_E \epsilon^{\frac{1}{2}} (\{\mathbf{q}_h\} - C_{11}[\![y_h]\!] - \mathbf{C}_{12}[\![\mathbf{q}_h]\!]) \cdot [\![v]\!] \, ds \\ & + \sum_{K \in \mathcal{T}_h} \int_K \alpha y_h v \, dx + \sum_{E \in \mathcal{E}_h^0} \int_E (\{\mathbf{y}_h\} + \mathbf{D}_{11} \cdot [\![y_h]\!]) \beta \cdot [\![v]\!] \, ds + \sum_{E \subset \Gamma^+} \int_E (\mathbf{n} \cdot \beta) y_h v \, ds \\ & + \sum_{E \in \mathcal{E}_h^\partial} \int_E \epsilon^{\frac{1}{2}} (\mathbf{q}_h \cdot \mathbf{n} - C_{11} y_h) v \, ds = \int_{\Omega} f v \, dx - \sum_{E \in \mathcal{E}_h^\partial} \int_E \epsilon^{\frac{1}{2}} C_{11} u_h v \, ds + \sum_{E \subset \Gamma^-} \int_E |\beta \cdot \mathbf{n}| u_h v \, ds, \end{aligned}$$

and

$$\begin{aligned} & \int_{\Omega} \mathbf{q}_h \cdot \mathbf{r} \, dx - \sum_{K \in \mathcal{T}_h} \int_K \epsilon^{\frac{1}{2}} y_h \nabla \cdot \mathbf{r} \, dx + \sum_{E \in \mathcal{E}_h^0} \int_E \epsilon^{\frac{1}{2}} (\{\mathbf{y}_h\} + \mathbf{C}_{12} \cdot [\![y_h]\!]) [\![\mathbf{r}]\!] \, ds \\ & = - \sum_{E \in \mathcal{E}_h^\partial} \int_E \epsilon^{\frac{1}{2}} u_h \mathbf{r} \cdot \mathbf{n} \, ds. \end{aligned}$$

It is convenient to define the following bi(linear) forms:

$$\begin{aligned} a_h(\mathbf{q}, \mathbf{r}) &:= \int_{\Omega} \mathbf{q} \cdot \mathbf{r} \, dx, \\ b_h(y, \mathbf{r}) &:= - \sum_{K \in \mathcal{T}_h} \int_K \epsilon^{\frac{1}{2}} y \nabla \cdot \mathbf{r} \, dx + \sum_{E \in \mathcal{E}_h^0} \int_E \epsilon^{\frac{1}{2}} (\{\mathbf{y}\} + \mathbf{C}_{12} \cdot [\![y]\!]) [\![\mathbf{r}]\!] \, ds, \\ c_h(y, v) &:= \sum_{K \in \mathcal{T}_h} \int_K (\alpha y v - y \beta \cdot \nabla v) \, dx + \sum_{E \in \mathcal{E}_h^0} \int_E (\{\mathbf{y}\} + \mathbf{D}_{11} \cdot [\![y]\!]) \beta \cdot [\![v]\!] \, ds \\ & - \sum_{E \in \mathcal{E}_h^0} \int_E \epsilon^{\frac{1}{2}} C_{11} [\![y]\!] \cdot [\![v]\!] \, ds + \sum_{E \subset \Gamma^+} \int_E (\mathbf{n} \cdot \beta) y v \, ds - \sum_{E \in \mathcal{E}_h^\partial} \int_E \epsilon^{\frac{1}{2}} C_{11} y v \, ds, \\ m_{h,1}(u, \mathbf{r}) &:= - \sum_{E \in \mathcal{E}_h^\partial} \int_E \epsilon^{\frac{1}{2}} u \mathbf{r} \cdot \mathbf{n} \, ds, \\ m_{h,2}(u, v) &:= - \sum_{E \in \mathcal{E}_h^\partial} \int_E \epsilon^{\frac{1}{2}} C_{11} u v \, ds + \sum_{E \subset \Gamma^-} \int_E |\beta \cdot \mathbf{n}| u v \, ds, \\ F(v) &:= \int_{\Omega} f v \, dx. \end{aligned}$$

By applying integration by parts over the first term in $b_h(\cdot, \cdot)$, we obtain

$$\begin{aligned} b_h(y, \mathbf{r}) &= - \sum_{K \in \mathcal{T}_h} \int_K \epsilon^{\frac{1}{2}} y \nabla \cdot \mathbf{r} dx + \sum_{E \in \mathcal{E}_h^0} \int_E \epsilon^{\frac{1}{2}} (\{y\} + \mathbf{C}_{12} \cdot [y]) [\mathbf{r}] ds \\ &= \sum_{K \in \mathcal{T}_h} \int_K \epsilon^{\frac{1}{2}} \nabla y \cdot \mathbf{r} dx - \sum_{K \in \mathcal{T}_h} \int_{\partial K} \epsilon^{\frac{1}{2}} y \mathbf{r} \cdot \mathbf{n} ds \\ &\quad + \sum_{E \in \mathcal{E}_h^0} \int_E \epsilon^{\frac{1}{2}} (\{y\} + \mathbf{C}_{12} \cdot [y]) [\mathbf{r}] ds. \end{aligned}$$

Then, by following straightforward computation

$$\sum_{K \in \mathcal{T}_h} \int_{\partial K} \epsilon^{\frac{1}{2}} y \mathbf{r} \cdot \mathbf{n} ds = \sum_{E \in \mathcal{E}_h^0 \cup \mathcal{E}_h^\partial} \int_E \{\mathbf{r}\} \cdot [\epsilon^{\frac{1}{2}} y] ds + \sum_{E \in \mathcal{E}_h^0} \int_E [\mathbf{r}] \cdot \{\epsilon^{\frac{1}{2}} y\} ds$$

we get

$$\begin{aligned} b_h(y, \mathbf{r}) &= \sum_{K \in \mathcal{T}_h} \int_K \epsilon^{\frac{1}{2}} \nabla y \cdot \mathbf{r} dx - \sum_{E \in \mathcal{E}_h^0} \int_E \epsilon^{\frac{1}{2}} (\{\mathbf{r}\} - \mathbf{C}_{12} [\mathbf{r}]) \cdot [y] ds \\ &\quad - \sum_{E \in \mathcal{E}_h^\partial} \int_E \epsilon^{\frac{1}{2}} y \mathbf{r} \cdot \mathbf{n} ds. \end{aligned}$$

For given right-hand side f and boundary condition u , the LDG approximation of the unique solution (y, \mathbf{q}) to (8a) is given by $(y_h, \mathbf{q}_h) \in V_h \times \mathbf{W}_h$ satisfying

$$a_h(\mathbf{q}_h, \mathbf{r}) + b_h(y_h, \mathbf{r}) = m_{h,1}(u, \mathbf{r}) \quad \forall \mathbf{r} \in \mathbf{W}_h, \quad (14a)$$

$$-b_h(v, \mathbf{q}_h) + c_h(y_h, v) = m_{h,2}(u, v) + F(v) \quad \forall v \in V_h. \quad (14b)$$

For given $u \in L^2(\Gamma)$ and $f \in L^2(\Omega)$, this system admits a unique solution, which can be shown using arguments similar to those in [14, Proposition 2.1].

Hence, the LDG approximation scheme of the Dirichlet boundary control problem (1)–(2) reads as

$$\underset{u_h \in U_h^{\text{ad}}, (y_h, \mathbf{q}_h) \in V_h \times \mathbf{W}_h}{\text{minimize}} \quad J(y_h, u_h) = \frac{1}{2} \|y_h - y^d\|_{0,\Omega}^2 + \frac{\omega}{2} \|u_h\|_{0,\Gamma}^2 \quad (15)$$

subject to

$$a_h(\mathbf{q}_h, \mathbf{r}) + b_h(y_h, \mathbf{r}) = m_{h,1}(u_h, \mathbf{r}) \quad \forall \mathbf{r} \in \mathbf{W}_h, \quad (16a)$$

$$-b_h(v, \mathbf{q}_h) + c_h(y_h, v) = m_{h,2}(u_h, v) + F(v) \quad \forall v \in V_h. \quad (16b)$$

Here, the set of admissible controls either is chosen as $U_h^{\text{ad}} := U^{\text{ad}}$, which is the case of variational discretization [31], or as $U_h^{\text{ad}} := U^{\text{ad}} \cap U_h$, which we refer to as the case of full discretization. Since U_h^{ad} is nonempty, closed, and convex and J is uniformly convex, problem (15)–(16) admits a unique solution $((y_h, \mathbf{q}_h), u_h) \in (V_h \times \mathbf{W}_h) \times U_h^{\text{ad}}$. Moreover, it follows from standard arguments that $((y_h, \mathbf{q}_h), u_h)$ is the unique solution of the optimal control problem (15)–(16) if and only if a pair $(\mathbf{p}_h, z_h) \in \mathbf{W}_h \times V_h$ of discrete adjoint flux and discrete adjoint potential exists, which together with $((y_h, \mathbf{q}_h), u_h, (\mathbf{p}_h, z_h))$ solves the following discrete optimality conditions

$$a_h(\mathbf{q}_h, \mathbf{r}) + b_h(y_h, \mathbf{r}) = m_{h,1}(u_h, \mathbf{r}), \quad \forall \mathbf{r} \in \mathbf{W}_h, \quad (17a)$$

$$-b_h(v, \mathbf{q}_h) + c_h(y_h, v) = m_{h,2}(u_h, v) + F(v), \quad \forall v \in V_h, \quad (17b)$$

$$a_h(\mathbf{p}_h, \psi) - b_h(z_h, \psi) = 0, \quad \forall \psi \in \mathbf{W}_h, \quad (17c)$$

$$b_h(\phi, \mathbf{p}_h) + c_h(\phi, z_h) = (y_h - y^d, \phi)_\Omega, \quad \forall \phi \in V_h, \quad (17d)$$

$$\langle \omega u_h + m'_{1,h}(u_h, \mathbf{p}_h) + m'_{2,h}(u_h, z_h), w - u_h \rangle_\Gamma \geq 0, \quad \forall w \in U_h^{\text{ad}}. \quad (17e)$$

The variational inequality in (17e) in terms of \mathbf{q}_h and z_h reads

$$\langle \omega u_h - \epsilon^{\frac{1}{2}} \mathbf{p}_h \cdot \mathbf{n} + \kappa_z z_h, w - u_h \rangle_{\Gamma} \geq 0, \quad \forall w \in U_h^{\text{ad}}, \quad (18)$$

where $\kappa_z = -\epsilon^{\frac{1}{2}} C_{11} + \chi_{\Gamma-} |\beta \cdot \mathbf{n}|$ with χ denoting the indicator function.

If the optimal solution $(y, \mathbf{q}, z, \mathbf{p}, u) \in V \times \mathbf{W} \times V \times \mathbf{W} \times U^{\text{ad}}$ is smooth enough, it also satisfies the system

$$a_h(\mathbf{q}, \mathbf{r}) + b_h(y, \mathbf{r}) = m_{h,1}(u, \mathbf{r}), \quad \forall \mathbf{r} \in \mathbf{W}, \quad (19a)$$

$$-b_h(v, \mathbf{q}) + c_h(y, v) = m_{h,2}(u, v) + F(v), \quad \forall v \in V, \quad (19b)$$

$$a_h(\mathbf{p}, \psi) - b_h(z, \psi) = 0, \quad \forall \psi \in \mathbf{W}, \quad (19c)$$

$$b_h(\phi, \mathbf{p}) + c_h(\phi, z) = (y - y^d, \phi)_{\Omega}, \quad \forall \phi \in V, \quad (19d)$$

$$\langle \omega u + m'_{1,h}(u, \mathbf{p}) + m'_{2,h}(u, z), w - u \rangle_{\Gamma} \geq 0, \quad \forall w \in U^{\text{ad}}. \quad (19e)$$

4 Error estimates

In this section, we present error estimates for the LDG approximation of the Dirichlet boundary control problem defined on a convex polygonal domain. The analysis is carried out for two different discretization strategies applied to the optimal control problem: the variational discretization approach and the piecewise linear discretization approach.

Let us introduce the control-to-state operator $S : L^2(\Gamma) \rightarrow H^{\frac{1}{2}}(\Omega)$, defined by $u \mapsto S(u) := y$, where for a given u the state y satisfies (4). Using this, the reduced cost functional can be written as

$$\widehat{J} : U \rightarrow \mathbb{R}, \quad \widehat{J}(u) = J(Su, u).$$

Hence, the optimal control problem (1)-(2) can be reformulated as

$$\min_{u \in U^{\text{ad}}} \widehat{J}(u). \quad (20)$$

Following standard arguments in [41], the existence and uniqueness of an optimal solution $u \in U^{\text{ad}}$ can be established by invoking the continuity and strict convexity of \widehat{J} . For a control $u \in U$ and a direction $\delta u \in U$, the directional derivatives are given by

$$\widehat{J}'(u)(\delta u) = (y - y^d, y(\delta u))_{\Omega} + \omega \langle u, \delta u \rangle_{\Gamma} = \langle \omega u - \epsilon^{\frac{1}{2}} \mathbf{p} \cdot \mathbf{n}, \delta u \rangle_{\Gamma}, \quad (21)$$

where y is the state associated to the control u , $y(\delta u)$ denotes the state assigned to the control δu , and \mathbf{p} is the adjoint flux associated to the observation $y - y^d$. The necessary optimality condition of the reduced problem (20) is given as a variational inequality:

$$\widehat{J}'(u)(\delta u - u) \geq 0 \quad \forall \delta u \in U^{\text{ad}}. \quad (22)$$

To discretize the reduced optimal control problem (20), we define the discrete reduced cost functional as

$$\widehat{J}_h : U \rightarrow \mathbb{R}, \quad \widehat{J}_h(u) = J(S_h u, u),$$

where $S_h : u \mapsto y_h(u)$ represents the discrete solution operator, which according to [14, Proposition 2.1] is well defined. The corresponding discretized reduced problem is then given by

$$\min_{u \in U_h^{\text{ad}}} \widehat{J}_h(u). \quad (23)$$

Analogous to the continuous case, the discrete reduced cost functional \widehat{J}_h is quadratic. Its directional derivative is given by

$$\widehat{J}'_h(u)(\delta u) = (y_h(u) - y^d, y_h(\delta u))_{\Omega} + \omega \langle u, \delta u \rangle_{\Gamma} = \langle \omega u - \epsilon^{\frac{1}{2}} \mathbf{p}_h \cdot \mathbf{n} + \kappa_z z_h, \delta u \rangle_{\Gamma}, \quad (24)$$

where $y_h(u)$, $y_h(\delta u)$ are denote discrete states associated to u and δu , respectively, and \mathbf{p}_h and z_h denote the adjoint flux and potential associated with $y_h(u) - y^d$.

In this work, we consider two approaches for the discretization of the control variable: the *variational discretization* proposed in [31], and the *piecewise linear discretization*. For the linear discretization, we employ the discrete space defined in (10), while in the case of variational discretization, the discrete control space is chosen as $U_h = U = L^2(\Gamma)$. In both settings, the discrete admissible control set is given by $U_h^{\text{ad}} = U_h \cap U^{\text{ad}}$. Furthermore, for the variational discretization approach, the discrete optimal control u_h is characterized by

$$\widehat{J}'_h(u_h)(\delta u - u_h) \geq 0, \quad \forall \delta u \in U^{\text{ad}}, \quad (25)$$

whereas for the linear discretization approach, the discrete optimal control u_h satisfies

$$\widehat{J}_h(u_h)(\delta u_h - u_h) \geq 0, \quad \forall \delta u_h \in U_h^{\text{ad}}. \quad (26)$$

In the analysis, we require an interpolation/projection operator that preserves admissibility; however, the L^2 -projection does not, in general, preserve the admissibility of functions in U^{ad} . Hence, we employ the quasi-interpolation operator $\pi_h : L^1(\partial\Omega) \rightarrow \mathcal{E}_h^\partial$ inspired by [10], and used in the context of Dirichlet boundary control, see, e.g., in [45]. The operator π_h is defined as

$$\pi_h u = \sum_{n \in \mathcal{N}_h^\partial} \frac{(u, \xi_n)}{(1, \xi_n)} \xi_n, \quad (27)$$

where \mathcal{N}_h^∂ denotes the set of all mesh nodes of \mathcal{T}_h lying on the boundary Γ , and $\xi_n \in U_h$ represents the local (nodal) basis function associated with node n on the boundary. By construction, it follows that $\pi_h u \in U_h^{\text{ad}}$ for every $u \in U^{\text{ad}}$. For $u \in H^s(\Gamma)$ with $0 \leq s \leq 1$, the following estimates also hold [45, Lemma 5.5]

$$\|u - \pi_h u\|_{0,\Gamma} \leq Ch^s \|u\|_{s,\Gamma}, \quad (28a)$$

$$\|u - \pi_h u\|_{-s,\Gamma} \leq Ch^{2s} \|u\|_{s,\Gamma}. \quad (28b)$$

In the numerical error analysis it will be convenient to use the adjoint representations of the respective derivatives \widehat{J}' and \widehat{J}'_h , where we already here note, that, due to $z = 0$ on Γ , we also can write

$$\widehat{J}'(u)(\delta u) = \langle \omega u - \epsilon^{\frac{1}{2}} \mathbf{p} \cdot \mathbf{n} + \kappa_z z, \delta u \rangle_\Gamma. \quad (29)$$

To facilitate the analysis, we also introduce the following auxiliary problem: find $(z_h(y), \mathbf{p}_h(y)) \in V_h \times \mathbf{W}_h$ such that

$$a_h(\mathbf{p}_h(y), \psi) - b_h(z_h(y), \psi) = 0, \quad \forall \psi \in \mathbf{W}_h, \quad (30a)$$

$$b_h(\phi, \mathbf{p}_h(y)) + c_h(\phi, z_h(y)) = (y - y^d, \phi)_\Omega, \quad \forall \phi \in V_h. \quad (30b)$$

Here, $(z_h(y), \mathbf{p}_h(y))$ denotes the LDG approximation of (z, \mathbf{p}) .

We begin by establishing an error estimate for the variational discretization.

Theorem 4.1. *Let u be the solution of (20), and let u_h be the corresponding discrete control obtained with the choice $U_h = U = L^2(\Gamma)$. Moreover, let y and y_h denote the corresponding continuous and discrete state solutions, respectively. Then,*

$$\omega \|u - u_h\|_{0,\Gamma}^2 + \|y - y_h\|_{0,\Omega}^2 \leq \|y - y_h(u)\|_{0,\Omega}^2 + C(\omega) (\epsilon \|(\mathbf{p}_h(u) - \mathbf{p}) \cdot \mathbf{n}\|_{0,\Gamma}^2 + \kappa_z^2 \|z_h(u) - z\|_{0,\Gamma}^2), \quad (31)$$

where the positive constant C is independent of the mesh size h , and where $\mathbf{p}_h(u) := \mathbf{p}_h(y(u), \mathbf{q}(u))$ and $z_h(u) := z_h(y(u), \mathbf{q}(u))$ are local discontinuous Galerkin approximations of \mathbf{p} and z associated with the continuous data $u, y(u)$, and $\mathbf{q}(u)$, respectively, i.e., $(z_h(u), \mathbf{p}_h(u))$ solves (17c)-(17d) with right hand side $y - y^d$.

Proof. By taking $\delta u = u_h$ in (22) and $\delta u = u$ in (25), we obtain

$$\langle \widehat{J}'(u_h) - \widehat{J}'(u), u - u_h \rangle \geq 0,$$

that is, since $z|_{\Gamma} = 0$,

$$\langle \omega(u_h - u) - \epsilon^{\frac{1}{2}}(\mathbf{p}_h - \mathbf{p}) \cdot \mathbf{n} + \kappa_z(z_h - z), u - u_h \rangle_{\Gamma} \geq 0.$$

Recalling the definition of $m_{h,1}$ and $m_{h,2}$ this implies

$$\begin{aligned} \omega \|u - u_h\|_{0,\Gamma}^2 &\leq m_{h,1}(u - u_h, \mathbf{p}_h - \mathbf{p}) + m_{h,2}(u - u_h, z_h - z) \\ &= m_{h,1}(u - u_h, \mathbf{p}_h - \mathbf{p}_h(u)) + m_{h,2}(u - u_h, z_h - z_h(u)) \\ &\quad + m_{h,1}(u - u_h, \mathbf{p}_h(u) - \mathbf{p}) + m_{h,2}(u - u_h, z_h(u) - z) \\ &=: I_1 + I_2. \end{aligned} \quad (32)$$

To derive a bound for I_1 in (32), we make use of the optimality conditions (17a)-(17d) together with Young's inequality

$$\begin{aligned} I_1 &= m_{h,1}(u - u_h, \mathbf{p}_h - \mathbf{p}_h(u)) + m_{h,2}(u - u_h, z_h - z_h(u)) \\ &= a_h(\mathbf{q}_h(u) - \mathbf{q}_h, \mathbf{p}_h - \mathbf{p}_h(u)) + b_h(y_h(u) - y_h, \mathbf{p}_h - \mathbf{p}_h(u)) \\ &\quad - b_h(z_h - z_h(u), \mathbf{q}_h(u) - \mathbf{q}_h) + c_h(y_h(u) - y_h, z_h - z_h(u)) \\ &= (y_h - y, y_h(u) - y_h)_{\Omega} = (y_h - y, y_h(u) - y + y - y_h)_{\Omega} \\ &\leq -\frac{1}{2} \|y - y_h\|_{0,\Omega}^2 + \frac{1}{2} \|y_h(u) - y\|_{0,\Omega}^2, \end{aligned} \quad (33)$$

where $y_h(u)$ denotes the local discontinuous Galerkin approximation of the state variable corresponding to the Dirichlet boundary condition u .

For I_2 we have

$$\begin{aligned} I_2 &= m_{h,1}(u - u_h, \mathbf{p}_h(u) - \mathbf{p}) + m_{h,2}(u - u_h, z_h(u) - z) \\ &\leq \frac{\omega}{2} \|u - u_h\|_{0,\Gamma}^2 + C(\omega) (\epsilon \|(\mathbf{p}_h(u) - \mathbf{p}) \cdot \mathbf{n}\|_{0,\Gamma}^2 + \kappa_z^2 \|z_h(u) - z\|_{0,\Gamma}^2). \end{aligned} \quad (34)$$

Combining (33) and (34) in (32), we obtain the estimate in (31). \square

For the fully discrete approach we have

Theorem 4.2. *Let u be the solution of (20) and u_h be the corresponding discrete control obtained with the choice of U_h defined in (10). Further, let y and y_h denote the corresponding continuous state discrete state, respectively. Then,*

$$\begin{aligned} \omega \|u - u_h\|_{0,\Gamma}^2 + \|y - y_h\|_{0,\Omega}^2 &\leq \|y - y_h(u)\|_{0,\Omega}^2 + C(\omega) (\epsilon \|(\mathbf{p}_h(u) - \mathbf{p}) \cdot \mathbf{n}\|_{0,\Gamma}^2 + \kappa_z^2 \|z_h(u) - z\|_{0,\Gamma}^2) \\ &\quad + C(\omega) \|\pi_h u - u\|_{0,\Gamma}^2 + (\epsilon^{1/2} \|(\mathbf{p}_h - \mathbf{p}(y_h)) \cdot \mathbf{n}\|_{0,\Gamma} + \kappa_z \|z_h - z(y_h)\|_{0,\Gamma}) \|\pi_h u - u\|_{0,\Gamma} \\ &\quad + C(\|u\|_{s,\Gamma}, \|\mathbf{p}(u) \cdot \mathbf{n}\|_{s,\Gamma}) \|\pi_h u - u\|_{-s,\Gamma}, \end{aligned} \quad (35)$$

where the triplet $(y_h(u), z_h(u), \mathbf{p}_h(u))$ denotes the local discontinuous Galerkin approximations of (y, z, \mathbf{p}) for the given $u \in H^s(\Gamma)$ ($0 \leq s \leq 1$), i.e., $(y_h(u), z_h(u), \mathbf{p}_h(u))$ solves (17a)-(17d) with the data u and $y - y^d$, and $(\mathbf{p}(y_h), z(y_h))$ denotes the continuous adjoint flux and potential associated to the optimal discrete state y_h , i.e., the solution to (8b) with right hand side $y_h - y^d$.

Proof. From the definitions of the variational inequalities and the quasi-interpolation property in (27), we have

$$\begin{aligned}\widehat{J}'(u)(u_h - u) &\geq 0 & \forall u_h \in U_h^{\text{ad}} = U_h \cap U^{\text{ad}} \subset U^{\text{ad}}, \\ \widehat{J}'_h(u_h)(\pi_h u - u_h) &\geq 0 & \forall \pi_h u \in U_h^{\text{ad}}.\end{aligned}$$

Adding these inequalities gives

$$\underbrace{(\widehat{J}'_h(u_h) - \widehat{J}'(u))(u - u_h)}_{(1)} + \underbrace{\widehat{J}'_h(u_h)(\pi_h u - u)}_{(2)} \geq 0. \quad (36)$$

We now can estimate (1) in (36) as in the proof of Theorem 4.1, which gives contributions to the upper part of (35). To treat (2) in (36) we write

$$\begin{aligned}J'_h(u_h)(\pi_h u - u) &= \langle \omega u_h - \epsilon^{\frac{1}{2}} \mathbf{p}_h \cdot \mathbf{n} + \kappa_z z_h, \pi_h u - u \rangle \\ &= \langle \omega(u_h - u), \pi_h u - u \rangle \\ &\quad + \langle \epsilon^{\frac{1}{2}} (\mathbf{p}(y_h) - \mathbf{p}_h) \cdot \mathbf{n} + \kappa_z(z_h - z(y_h)), \pi_h u - u \rangle \\ &\quad + \langle \epsilon^{\frac{1}{2}} (\mathbf{p}(u) - \mathbf{p}(y_h)) \cdot \mathbf{n} + \kappa_z(z(y_h) - z(u)), \pi_h u - u \rangle \\ &\quad + \langle \omega u - \epsilon^{\frac{1}{2}} \mathbf{p}(u) \cdot \mathbf{n} + \kappa_z z(u), \pi_h u - u \rangle.\end{aligned} \quad (37)$$

Here, $\mathbf{p}(u), z(u)$ denote the optimal adjoint flux and adjoint potential, respectively, while $\mathbf{p}(y_h), z(y_h)$ denote auxiliary continuous adjoint flux and potential associated to the optimal discrete adjoint state y_h , i.e., with right hand side $y_h - y^d \in L^2(\Omega)$ in (8b). We already note at this stage of the proof that the continuous adjoint variables z are zero on the boundary. Straightforward estimation gives

$$\begin{aligned}J'_h(u_h)(\pi_h u - u) &\leq \frac{\omega}{4} \|u - u_h\|_{0,\Gamma}^2 + C(\omega) \|\pi_h u - u\|_{0,\Gamma}^2 \\ &\quad + C(\epsilon^{1/2} \|(\mathbf{p}_h - \mathbf{p}(y_h)) \cdot \mathbf{n}\|_{0,\Gamma} + \kappa_z \|z_h - z(y_h)\|_{0,\Gamma}) \|\pi_h u - u\|_{0,\Gamma} \\ &\quad + C\epsilon^{1/2} \|(\mathbf{p}(y_h) - \mathbf{p}(u)) \cdot \mathbf{n}\|_{0,\Gamma} \|\pi_h u - u\|_{0,\Gamma} \\ &\quad + C\|(\omega u - \epsilon^{1/2} \mathbf{p}(u) \cdot \mathbf{n})\|_{s,\Gamma} \|\pi_h u - u\|_{-s,\Gamma}.\end{aligned} \quad (38)$$

Since $y_h, y^d \in L^2(\Omega)$ we have $z(y_h) \in H^2(\Omega) \cap H_0^1(\Omega)$. The trace theorem together with the continuity of the continuous adjoint solution operator gives

$$\|(\mathbf{p}(y_h) - \mathbf{p}(u)) \cdot \mathbf{n}\|_{0,\Gamma} \leq C \|z(y_h) - z(u)\|_{2,\Omega} \leq C \|y_h - y\|_{0,\Omega}, \quad (39)$$

so that

$$C\epsilon^{1/2} \|(\mathbf{p}(y_h) - \mathbf{p}(u)) \cdot \mathbf{n}\|_{0,\Gamma} \|\pi_h u - u\|_{0,\Gamma} \leq \frac{1}{4} \|y - y_h\|_{0,\Omega}^2 + C \|\pi_h u - u\|_{0,\Gamma}^2.$$

Sorting the addends of (38) in accordingly gives the estimate (35). \square

Discussion of Theorem 4.1 and Theorem 4.2: In both cases, the variational discrete and the fully discrete case, to obtain error estimates for the optimal control and the associated state we need LDG error estimates for the state, the adjoint flux as well as for the adjoint potential under natural regularity requirements on the continuous optimal control u and the data y^d (and f).

Let us first recall what is known from literature w.r.t. the approximation properties of LDG approximations. In the first instance we here use results of [14]. From there with Theorem 2.1, Table 2.1 and 4.1 one obtains for the case $k = 1$:

Lemma 4.3. *Let $(v, \mathbf{w}) \in V \times \mathbf{W}$ be the solutions of (9) and let $(v_h, \mathbf{w}_h) \in V_h \times \mathbf{W}_h$ be its LDG approximation, i.e., the solution of the discretized problem (16). Assume that $v \in H^{s+2}(\Omega)$ for some $s \geq 0$. Then*

$$|v - v_h|_{1,\Omega} + \|\mathbf{w} - \mathbf{w}_h\|_{0,\Omega} \leq Ch\|v\|_{2,\Omega}. \quad (40)$$

Moreover, the following L^2 -error bound holds

$$\|v - v_h\|_{0,\Omega} \leq Ch^2\|v\|_{2,\Omega}. \quad (41)$$

If one inspects the proof of this Lemma, one recognizes that higher regularity of $(v, \mathbf{w}) \in H^{s+2}(\Omega) \times H^{s+2}(\Omega)^2$ for $s \in (0, 1)$ in our case $k = 1$ does not affect the error estimate. If we look at the variables of our optimization problem we observe, that for $y^d \in L^2(\Omega)$ (and $u \in H^{1/2}(\Gamma)$, which is the minimal regularity we obtain for the control u), the adjoint potential satisfies $z \in H^2(\Omega) \cap H_0^1(\Omega)$ with flux $\mathbf{p} \in H^1(\Omega, \mathbb{R}^2)$. In this case we conclude

$$\kappa_z\|z(u) - z_h(u)\|_{0,\Gamma} \sim h^{1/2}, \quad \|\mathbf{p}(u) \cdot \mathbf{n} - \mathbf{p}_h(u) \cdot \mathbf{n}\|_{0,\Gamma} \sim h^{1/2},$$

since in our LDG method $C_{11} \sim h^{-1}$. Moreover, with Lemma 4.3 we for higher regularity of the involved variables according to Theorem 2.2 may not expect an improvement for the case $k = 1$. But we only have $y \in H^1(\Omega)$ with flux $\mathbf{q} \in H(\text{div}, \Omega)$. With this, Lemma 4.3 is not applicable. However, in Lemma 4.3 of the recent paper [37] treating stability and convergence of the HDG method in approximating solutions to elliptic PDEs, it among other things is shown that for $s \in [0, 1]$

$$\|y - y_h(u)\|_{0,\Omega} \leq Ch^{s+1}|y|_{H^{s+1}(\Omega)} \quad (42)$$

holds. Adapting this result to our setting we may expect to have the error behaviour

$$\|u - u_h\|_{0,\Gamma} + \|y - y_h\|_{0,\Omega} \sim h + h^{1/2} + h^{1/2} \sim h^{1/2}.$$

This compares very well to the results of [27] for the case $k = 0$, that is, piecewise constant flux and piecewise linear potential approximation.

In the fully discrete case, additional terms to estimate occur. For the error with the quasi-interpolation operator π_h one has for $u \in H^s(\Gamma)$ and $0 \leq s \leq 1$ from (28a)-(28b)

$$\|u - \pi_h u\|_{0,\Gamma} \sim h^s \quad \text{and} \quad \|u - \pi_h u\|_{-s,\Gamma} \sim h^{2s}.$$

For the generic case $s = \frac{1}{2}$ this gives the convergence behaviour $h^{1/2}$ and h^1 , respectively. We also need to estimate the approximation errors for $\mathbf{p}(y_h)$ and $z(y_h)$, where y_h denotes the discrete optimal potential. Since $y_h \in L^2(\Omega)$ with

$$\|y_h\|_{0,\Omega} \leq C$$

uniformly in h (this directly follows from $\|y_h\|_{0,\Omega} \leq \sqrt{4\hat{J}_h(0) + 2\|y^d\|_{0,\Omega}^2}$) we conclude with Lemma 4.3

$$\|(\mathbf{p}_h - \mathbf{p}(y_h)) \cdot \mathbf{n}\|_{0,\Gamma} + \kappa_z\|z_h - z(y_h)\|_{0,\Gamma} \sim h^{1/2}.$$

Finally, since $\mathbf{p} \cdot \mathbf{n} \in H^{1/2}(\Gamma)$ (see e.g. [2]) we may apply (28b) with $s = \frac{1}{2}$. All together, we for $u \in H^{1/2}$ also in the fully discrete case obtain the error behaviour

$$\|u - u_h\|_{0,\Gamma} + \|y - y_h\|_{0,\Omega} \sim h^{1/2}.$$

Remark 4.4. *We note that in the work of Cockburn et al. [19] error analysis for a LDG scheme is presented, which fits to our setting of Section 3. From Theorem 2.1 in combination with Theorems 3.1 and 4.1 of this work it is possible to deduce the error estimates*

$$\|y - y_h\|_{0,\Omega} \leq C \{ h^{l_y+1}|y|_{l_y+1,\Omega} + h^{l_q+2}(|\text{div } \mathbf{q}|_{l_q,\Omega} + |\mathbf{q}|_{l_q+1,\Omega}) \}$$

and

$$\|\mathbf{q} - \mathbf{q}_h\|_{0,\Omega} \leq C \{ h^{l_y} |y|_{l_y+1,\Omega} + h^{l_q+1} |\mathbf{q}|_{l_q+1,\Omega} \},$$

where $l_y, l_q \in [0, k]$ with k denoting the polynomial degree in our LDG scheme. In the present work, we use $k = 1$. In this version, at least fluxes in $H^1(\Omega)$ are required and we obtain a more detailed version of the estimate of Lemma 4.3. In our present optimal control setting we only have generic regularity $\mathbf{q} \in H(\text{div}, \Omega)$ of the optimal flux and $y \in H^1(\Omega)$ for the optimal potential. Utilizing the fact that $\mathbf{q} \cdot \mathbf{n} \in H^{-1/2}(\Gamma)$ in the definition of the respective projections we think that it is possible to extend the proof of [19, Theorem 2.1] to our generic regularity setting, yielding the error estimates

$$\|y - y_h\|_{0,\Omega} \leq C \{ h^{l_y+1} |y|_{l_y+1,\Omega} + h^{l_q+1} (|\text{div } \mathbf{q}|_{l_q,\Omega} + |\mathbf{q}|_{l_q \cap H(\text{div}),\Omega}) \} \quad (43)$$

and

$$\|\mathbf{q} - \mathbf{q}_h\|_{0,\Omega} \leq C \{ h^{l_y} |y|_{l_y+1,\Omega} + h^{l_q} |\mathbf{q}|_{l_q \cap H(\text{div}),\Omega} \}, \quad (44)$$

where again $l_q, l_y \in [0, k]$. For the case $k = 1$ and $u \in H^{1/2}(\Omega)$ we for $l_y = l_q = 0$ then get the estimate

$$\|y - y_h\|_{0,\Omega} \leq Ch \{ |y|_{1,\Omega} + |q|_{H(\text{div}),\Omega} \} \quad (45)$$

together with a stability estimate for \mathbf{q}_h . It is then possible to replace the estimate (42) in our convergence discussion by that of (45). Moreover, only $\mathbf{q} \in H^{l_q}(\Omega) \cap H(\text{div}, \Omega)$ is required. However, in the case $k = 1$ estimates (43)-(44) do not deliver improved error estimates for the errors in optimal control and state, since the regularity of the adjoint variables obtained for $s \in [\frac{1}{2}, \frac{3}{2})$ from Theorem 2.2 does not contribute to improved convergence order in the case $k = 1$. This only would pay off for $k \geq 2$, compare also the case $k \geq 1$ of [27] which would relate to the case $k \geq 2$ of our setting. We leave it to the interested reader to inspect the details.

5 Numerical Experiments

In this section, we provide numerical experiments to demonstrate the performance of the local discontinuous Galerkin discretization and to underpin the theoretical findings established for the Dirichlet boundary control problems. All numerical results are obtained using piecewise linear approximations for the state y , the state flux \mathbf{q} , the adjoint z , the adjoint flux \mathbf{p} , and the control u . The mesh is generated by partitioning Ω into $n \times n$ uniform squares and subdividing each square into two triangles. To solve the discretized control constrained problem the primal-dual active set algorithm is applied as a semismooth Newton step; see, e.g., [8]. The optimization procedure is terminated when two consecutive active sets coincide. Moreover, the experimental order of convergence is computed using

$$\text{rate} = \frac{1}{\ln 2} \ln \left(\frac{\|e(h)\|_{0,\Omega}}{\|e(h/2)\|_{0,\Omega}} \right),$$

where $e(h)$ denotes the error associated with a triangulation of mesh size h .

5.1 Example 1

Our first example is a modified form of the elliptic problem in [43] and represents an unconstrained problem with analytical solutions. The problem data are chosen as

$$\Omega = [0, 1] \times [0, 1], \quad \beta = (1, 1)^T, \quad \alpha = 1, \quad \omega = 1.$$

The source function $f(x_1, x_2)$ and the desired state $y^d(x_1, x_2)$ are generated so that the analytical solutions for the state y , adjoint z , and control u are given by

$$\begin{aligned} y(x_1, x_2) &= -\frac{\epsilon^{1/2}}{\omega} (x_1(1-x_1) + x_2(1-x_2)), \\ z(x_1, x_2) &= \epsilon^{-1/2} x_1 x_2 (1-x_1)(1-x_2), \\ u(x_1, x_2) &= -\frac{\epsilon^{1/2}}{\omega} (x_1(1-x_1) + x_2(1-x_2)), \end{aligned}$$

respectively.

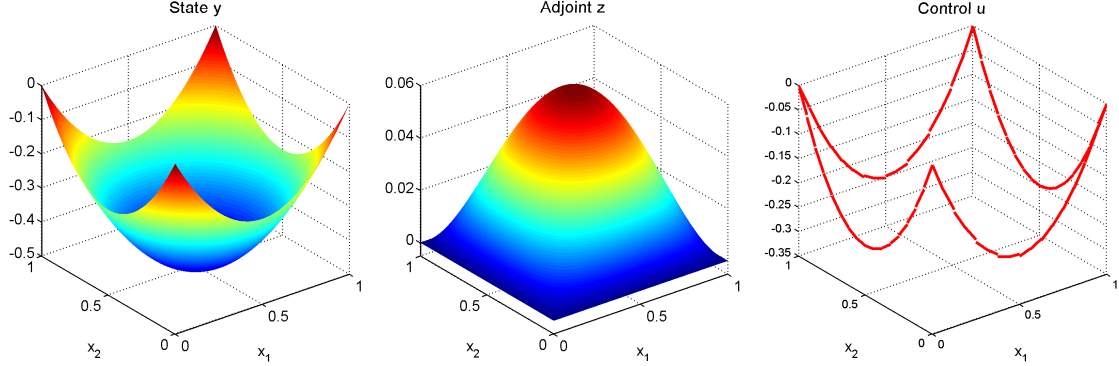


Figure 1: Example 5.1: Computed solutions of state y , adjoint z , and control u (from left to right) with $\epsilon = 1$.

Table 1: Example 5.1: Errors and convergence rates with $\epsilon = 1$.

# elements	$\ y - y_h\ _{0,\Omega}$	rate	$\ u - u_h\ _{0,\Gamma}$	rate	$\ z - z_h\ _{0,\Gamma}$	rate	$\ (\mathbf{p} - \mathbf{p}_h) \cdot \mathbf{n}\ _{0,\Gamma}$	rate
32	1.64e-02	-	4.27e-02	-	2.17e-02	-	1.03e-01	-
128	3.73e-03	2.14	2.14e-02	1.00	5.24e-03	2.05	5.53e-02	0.90
512	9.97e-04	1.90	1.12e-02	0.94	1.28e-03	2.03	2.91e-02	0.93
2048	3.00e-04	1.73	5.80e-03	0.95	3.13e-04	2.03	1.49e-02	0.97
8192	9.73e-05	1.62	2.97e-03	0.97	7.73e-05	2.02	7.52e-03	0.99
32768	3.29e-05	1.56	1.50e-03	0.98	1.92e-05	2.01	3.78e-03	0.99

Table 2: Example 5.1: Errors and convergence rates with $\epsilon = 10^{-6}$.

# elements	$\ y - y_h\ _{0,\Omega}$	rate	$\ u - u_h\ _{0,\Gamma}$	rate	$\ z - z_h\ _{0,\Gamma}$	rate	$\ (\mathbf{p} - \mathbf{p}_h) \cdot \mathbf{n}\ _{0,\Gamma}$	rate
32	3.87e-02	-	7.39e-02	-	6.63e+00	-	8.43e-02	-
128	5.33e-03	2.86	1.01e-02	2.88	1.80e+00	1.88	4.54e-02	0.89
512	8.50e-04	2.65	1.54e-03	2.71	4.70e-01	1.94	2.35e-02	0.95
2048	1.67e-04	2.35	2.90e-04	2.41	1.20e-01	1.97	1.20e-02	0.97
8192	4.49e-05	1.90	7.88e-05	1.88	3.03e-02	1.99	6.05e-03	0.99
32768	1.99e-05	1.17	3.99e-05	0.98	7.62e-03	1.99	3.04e-03	0.99

Figure 1 shows the computed solutions of the state y , adjoint z , and control u on a fine mesh with 32768 elements. Tables 1 and 2 present the $L^2(\Omega)$ errors of the state variable y , as well as the $L^2(\Gamma)$ errors of the control u , the adjoint state z , and the adjoint flux \mathbf{p} , corresponding to $\epsilon = 1$ and $\epsilon = 10^{-6}$, respectively. We observe that our scheme in the present example behaves stable with respect to ϵ . From the numerical computations, we observe higher convergence rates for $\|u - u_h\|_{0,\Gamma}$, $\|z - z_h\|_{0,\Gamma}$, and for $\|(\mathbf{p} - \mathbf{p}_h) \cdot \mathbf{n}\|_{0,\Gamma}$ than those expected by the theoretical analysis, whereas the rate for $\|y - y_h\|_{0,\Omega}$ is in accordance with Lemma 4.3.

5.2 Example 2

The following example, posed on the unit square $\Omega = [0, 1] \times [0, 1]$, is adopted from [13, 30] and does not admit an explicit analytical solution. The remaining problem data are specified as

$$f = 0, \quad y^d = \frac{1}{(x_1^2 + x_2^2)^{1/3}}, \quad \beta = (1, 1)^T, \quad \alpha = 1, \quad \omega = 1.$$

The admissible control set is defined by

$$U^{\text{ad}} = \{u \in L^2(\Gamma) : 0 \leq u(x) \leq 0.2 \text{ a.e. } x \in \Gamma\}.$$

Here, the largest interior angle is $\theta = \frac{\pi}{2}$ and $y^d \in H^{1/3-\eta}(\Omega)$ for any $\eta > 0$ due to the singularity on the boundary. Consequently, from Theorem 2.2, it follows that $s \in [\frac{1}{2}, \frac{5}{6}]$.

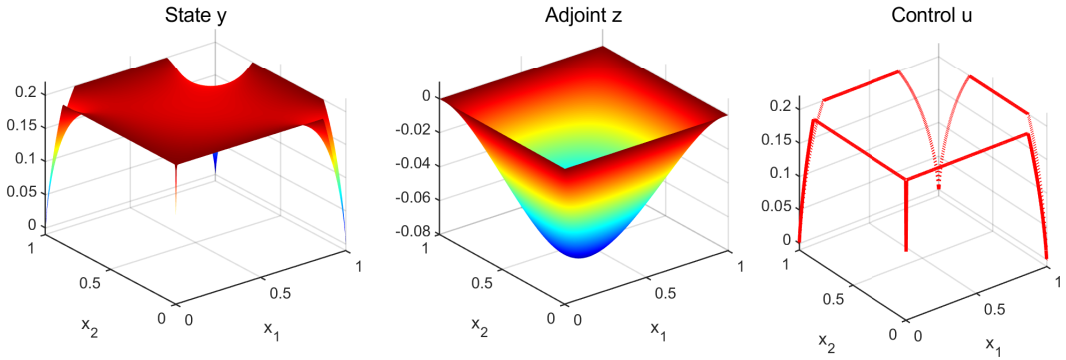


Figure 2: Example 5.2: Computed solutions of state y and adjoint z with $\epsilon = 1$.

Table 3: Example 5.2: Errors and convergence rates with $\epsilon = 1$.

# elements	$\ y - y_h\ _{0,\Omega}$	rate	$\ u - u_h\ _{0,\Gamma}$	rate	$\ z - z_h\ _{0,\Gamma}$	rate	$\ (\mathbf{p} - \mathbf{p}_h) \cdot \mathbf{n}\ _{0,\Gamma}$	rate
32	3.09e-02	-	1.14e-01	-	2.41e-02	-	1.78e-01	-
128	1.34e-02	1.21	6.57e-02	0.79	6.96e-03	1.79	1.11e-01	0.69
512	5.85e-03	1.20	3.37e-02	0.96	1.86e-03	1.91	6.40e-02	0.79
2048	2.54e-03	1.20	1.72e-02	0.97	4.83e-04	1.94	3.51e-02	0.87
8192	1.19e-03	1.10	9.47e-03	0.86	1.22e-04	1.99	1.81e-02	0.96
32768	5.29e-04	1.16	5.49e-03	0.79	2.59e-05	2.23	8.23e-03	1.14

Table 4: Example 5.2: Errors and convergence rates with $\epsilon = 10^{-4}$.

# elements	$\ y - y_h\ _{0,\Omega}$	rate	$\ u - u_h\ _{0,\Gamma}$	rate	$\ z - z_h\ _{0,\Gamma}$	rate	$\ (\mathbf{p} - \mathbf{p}_h) \cdot \mathbf{n}\ _{0,\Gamma}$	rate
32	7.23e-02	-	1.90e-01	-	2.00e-01	-	8.96e+00	-
128	4.32e-02	0.74	1.22e-01	0.65	1.45e-01	0.46	8.81e+00	0.03
512	2.46e-02	0.81	8.05e-02	0.59	1.15e-01	0.34	8.50e+00	0.05
2048	1.28e-02	0.94	5.44e-02	0.57	9.51e-02	0.28	7.87e+00	0.11
8192	6.52e-03	0.98	3.49e-02	0.64	7.52e-02	0.34	6.66e+00	0.24
32768	3.38e-03	0.95	1.77e-02	0.98	4.69e-02	0.68	4.32e+00	0.62

The problem is solved numerically on a fine mesh consisting of 131072 elements, and the resulting solution is used as a reference for comparison with solutions computed on coarser meshes. Figure 2 displays the numerical solutions computed on the reference mesh with $\epsilon = 1$. The

numerical results reported in Table 3 for $\epsilon = 1$ again show higher convergence rates for $\|u - u_h\|_{0,\Gamma}$, $\|z - z_h\|_{0,\Gamma}$, and for $\|(\mathbf{p} - \mathbf{p}_h) \cdot \mathbf{n}\|_{0,\Gamma}$ than those expected by the theoretical analysis, whereas the rate for $\|y - y_h\|_{0,\Omega}$ is in accordance with (43) with $l_y = 0$. Let us note that similar observations are also reported for a related example in [27, Tab.4], which corresponds to our numerical setting. However, the numerical results reported in Table 4 for $\epsilon = 10^{-4}$ show a convergence behaviour close to that reported in our numerical analysis.

5.3 Example 3

Our last example, adapted from [43], is formulated on a polygonal domain with maximum interior angle $\theta = \frac{5}{6}\pi$, as depicted in Figure 3. The remaining problem data are

$$y^d = \begin{cases} -1, & 0 \leq x_2 < 0.5, \\ 1, & 0.5 \leq x_2 < 1, \end{cases} \quad f = 1, \quad \beta = (1, 0)^T, \quad \alpha = 2, \quad \omega = 1.$$

The admissible control set is defined as

$$U^{\text{ad}} = \{u \in L^2(\Gamma) : 0 \leq u(x) \text{ a.e. } x \in \Gamma\}.$$

In this example, $y^d \in H^{1/2-\eta}(\Omega)$ for any $\eta > 0$ and the maximum interior angle is $\theta = \frac{5\pi}{6}$. Consequently, it follows that $s = [\frac{1}{2}, \frac{7}{10}]$ from Theorem 2.2.

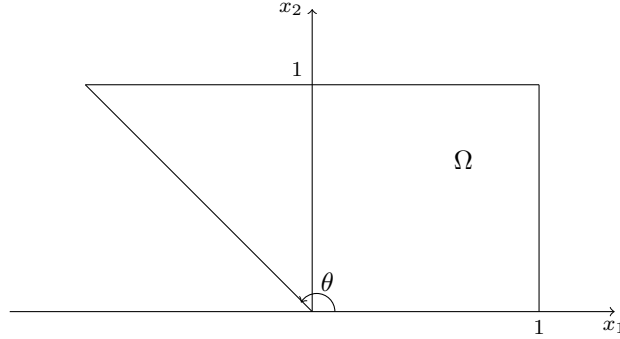


Figure 3: Example 5.3: Domain with $\theta = \frac{5}{6}\pi$.

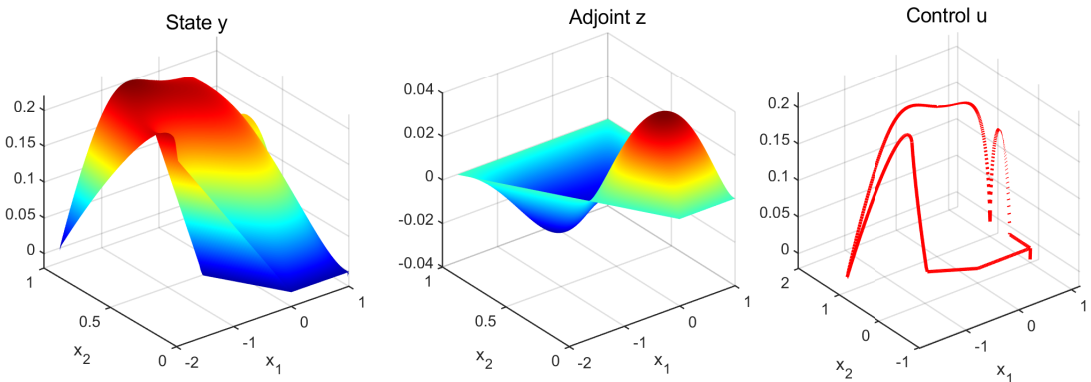


Figure 4: Example 5.3: Computed solutions of state y and adjoint z with $\epsilon = 1$.

Table 5: Example 5.3: Errors and convergence rates with $\epsilon = 1$.

# elements	$\ y - y_h\ _{0,\Omega}$	rate	$\ u - u_h\ _{0,\Gamma}$	rate	$\ z - z_h\ _{0,\Gamma}$	rate	$\ (\mathbf{p} - \mathbf{p}_h) \cdot \mathbf{n}\ _{0,\Gamma}$	rate
32	7.77e-02	-	1.86e-01	-	1.05e-01	-	3.34e-01	-
48	3.51e-02	1.15	1.02e-01	0.86	1.64e-02	2.69	1.46e-01	1.20
192	1.69e-02	1.05	5.66e-02	0.85	4.82e-03	1.76	8.13e-02	0.84
768	8.29e-03	1.02	2.81e-02	1.01	1.35e-03	1.84	4.33e-02	0.91
3072	4.03e-03	1.04	1.32e-02	1.09	3.45e-04	1.97	2.18e-02	0.99
12288	1.80e-03	1.16	5.53e-03	1.26	7.27e-05	2.25	9.65e-03	1.18

 Table 6: Example 5.3: Errors and convergence rates with $\epsilon = 10^{-4}$.

# elements	$\ y - y_h\ _{0,\Omega}$	rate	$\ u - u_h\ _{0,\Gamma}$	rate	$\ z - z_h\ _{0,\Gamma}$	rate	$\ (\mathbf{p} - \mathbf{p}_h) \cdot \mathbf{n}\ _{0,\Gamma}$	rate
32	1.17e-01	-	5.40e-02	-	5.28e-01	-	5.14e+00	-
48	7.62e-02	0.62	4.17e-02	0.37	5.14e-01	0.04	5.04e+00	0.03
192	5.43e-02	0.49	3.31e-02	0.33	4.99e-01	0.04	4.84e+00	0.06
768	4.36e-02	0.32	2.70e-02	0.30	4.59e-01	0.12	4.46e+00	0.12
3072	3.55e-02	0.30	2.12e-02	0.35	3.40e-01	0.43	3.75e+00	0.25
12288	2.38e-02	0.58	1.28e-02	0.72	1.46e-01	1.22	2.43e+00	0.63

The reference solutions have been computed on a fine mesh with 49152 elements; see Figure 4 with $\epsilon = 1$. For the convergence rates we obtain similar results as reported in the previous example, see Table 5 for $\epsilon = 1$ and Table 6 for $\epsilon = 10^{-4}$.

6 Conclusions

In this work, we have investigated Dirichlet boundary control for a convection–diffusion equation with L^2 -boundary controls subject to pointwise constraints, discretized using the LDG method. The LDG framework naturally incorporates the Dirichlet boundary conditions into the variational formulation, even when the control space is chosen as $L^2(\Gamma)$. We have derived general priori error estimates for the fully discrete and the variational discrete approximation of the optimal control problem in convex polygonal domains and presented numerical results that underpin the theoretical predictions, even for small values of the diffusion parameter ϵ . As future work, the development of a posteriori error estimates and adaptive discontinuous Galerkin methods could help to further robustify the numerical treatment in the convection dominated case.

References

- [1] R. A. Adams. *Sobolev Spaces*. Academic Press, Orlando, San Diego, New-York, 1975.
- [2] T. Apel, M. Mateos, J. Pfefferer, and A. Rösch. On the regularity of the solutions of Dirichlet optimal control problems in polygonal domains. *SIAM J. Control Optim.*, 53(6):3620–3641, 2015.
- [3] T. Apel, M. Mateos, J. Pfefferer, and A. Rösch. Error estimates for Dirichlet control problems in polygonal domains: quasi–uniform meshes. *Math. Control and Relat. F.*, 8(1):217–245, 2018.
- [4] N. Arada, E. Casas, and F. Tröltzsch. Error estimates for the numerical approximation of a semilinear elliptic control problem. *Comput. Optim. Appl.*, 23(2):201–229, 2002.
- [5] N. Arada and J.-P. Raymond. Dirichlet boundary control of semilinear parabolic equations. I. Problems with no state constraints. *Appl. Math. Optim.*, 45(2):125–143, 2002.

- [6] F. B. Belgacem, H. E. Fekih, and H. Metoui. Singular perturbation for the Dirichlet boundary control of elliptic problems. *M2AN Math. Model. Numer. Anal.*, 37:883–850, 2003.
- [7] P. Benner and H. Yücel. Adaptive symmetric interior penalty Galerkin method for boundary control problems. *SIAM J. Numer. Anal.*, 55(2):1101–1133, 2017.
- [8] M. Bergounioux, K. Ito, and K. Kunisch. Primal-dual strategy for constrained optimal control problems. *SIAM J. Control Optim.*, 37(4):1176–1194, 1999.
- [9] A. Buffa, T. J. R. Hughes, and G. Sangalli. Analysis of a multiscale discontinuous Galerkin method for convection-diffusion problems. *SIAM J. Numer. Anal.*, 44(4):1420–1440, 2006.
- [10] C. Carstensen. Quasi-interpolation and a posteriori error analysis in finite element methods. *ESAIM:M2AN*, 36:1197–1202, 1999.
- [11] E. Casas and M. Mateos. Error estimates for the numerical approximation of Neumann control problems. *Comput. Optim. Appl.*, 39(3):265–295, 2008.
- [12] E. Casas, M. Mateos, and J.-P. Raymond. Penalization of Dirichlet optimal control problems. *ESAIM Control Optim. Calc. Var.*, 15:782–809, 2009.
- [13] E. Casas and J.-P. Raymond. Error estimates for the numerical approximation of Dirichlet boundary control for semilinear elliptic equations. *SIAM J. Control Optim.*, 45(5):1586–1611, 2006.
- [14] P. Castillo, B. Cockburn, I. Pergugia, and D. Schötzau. An a priori error analysis of the local discontinuous Galerkin method for elliptic problems. *SIAM J. Numer. Anal.*, 38:1676–1706, 2000.
- [15] P. Castillo, B. Cockburn, D. Schötzau, and C. Schwab. Optimal a priori error estimates for the hp-version of the local discontinuous Galerkin method for convection-diffusion problems. *Math. Comp.*, 71:455–478, 2002.
- [16] H. Chen, J. R. Singler, and Y. Zhang. An HDG method for Dirichlet boundary control of convection dominated diffusion PDEs. *SIAM J. Numer. Anal.*, 57(4):1919–1946, 2019.
- [17] Y. Cheng and C.-W. Shu. Superconvergence of discontinuous Galerkin and local discontinuous Galerkin schemes for linear hyperbolic and convection-diffusion equations in one space dimension. *SIAM J. Numer. Anal.*, 47(6):4044–4072, 2010.
- [18] S. Chowdhury, T. Gudi, and A. K. Nandakumaran. Error bounds for a Dirichlet boundary control problem based on energy spaces. *Math. Comput.*, 86:1103–1126, 2017.
- [19] B. Cockburn, J. Gopalakrishnan, and F. J. Sayas. A projection-based error analysis of HDG methods. *Math. Comp.*, 79(271):1351–1367, 2010.
- [20] B. Cockburn and C.-W. Shu. The local discontinuous Galerkin method for time-dependent convection-diffusion systems. *SIAM J. Numer. Anal.*, 35:2440–2463, 1998.
- [21] B. Cockburn, G. Kanschat, and D. Schötzau. The local discontinuous Galerkin method for the Oseen equations. *Math. Comp.*, 73(246):569–593, 2004.
- [22] C. Corekli. The SIPG method of Dirichlet boundary optimal control problems with weakly imposed boundary conditions. *AIMS Math.*, 7(4):6711–6742, 2022.
- [23] K. Deckelnick, A. Günther, and M. Hinze. Finite element approximation of Dirichlet boundary control for elliptic PDEs on two- and three-dimensional curved domains. *SIAM J. Control Optim.*, 48:2798–2819, 2009.

- [24] S. Du and X. He. Finite element approximation to optimal Dirichlet boundary control problem: A priori and a posteriori error estimates. *Comput. Math. Appl.*, 131:14–25, 2023.
- [25] A. V. Fursikov, M. D. Gunzburger, and L. S. Hou. Boundary value problems and optimal boundary control for the Navier–Stokes systems: The two–dimensional case. *SIAM J. Control Optim.*, 36:852–894, 1998.
- [26] T. Geveci. On the approximation of the solution of an optimal control problem governed by an elliptic equation. *RAIRO Anal. Numer.*, 13:313–328, 1979.
- [27] W. Gong, W. Hu, M. Mateos, J. Singler, X. Zhang, and Y. Zhang. A new HDG method for Dirichlet boundary control of convection diffusion PDEs II: Low regularity. *SIAM J. Numer. Anal.*, 56(4):2262–2287, 2018.
- [28] W. Gong, W. Hu, M. Mateos, J. R. Singler, and Y. Zhang. Analysis of a hybridizable discontinuous Galerkin scheme for the tangential control of the Stokes system. *ESAIM: M2AN*, 54(6):2229–2264, 2020.
- [29] W. Gong, M. Mateos, J. Singler, and Y. Zhang. Analysis and approximations of Dirichlet boundary control of Stokes flows in the energy space. *SIAM J. Numer. Anal.*, 60(1):450–474, 2022.
- [30] W. Gong and N. Yan. Mixed finite element method for Dirichlet boundary control problem governed by elliptic PDEs. *SIAM J. Control Optim.*, 49(3):984–1014, 2011.
- [31] M. Hinze. A variational discretization concept in control constrained optimization: the linear-quadratic case. *Comput. Optim. Appl.*, 30:45–63, 2005.
- [32] M. Hinze and K. Kunisch. Second order methods for boundary control of the instationary Navier–Stokes system. *ZAMM Z. Angew. Math. Mech.*, 84:171–187, 2004.
- [33] M. Hinze and U. Matthes. A note on variational discretization of elliptic Neumann boundary control. *Control Cybern.*, 38(3):577–591, 2009.
- [34] M. Hinze, R. Pinna, M. Ulbrich, and S. Ulbrich. *Optimization with Partial Differential Equations*, volume 23 of *Mathematical Modelling, Theory and Applications*. Springer, Heidelberg, 2009.
- [35] W. Hu, M. Mateos, J. Singler, and Y. Zhang. A new HDG method for Dirichlet boundary control of convection diffusion PDEs I: High regularity. Technical report, 2018. arXiv:1801.01461v1.
- [36] W. W. Hu, J.G. Shen, J. R. Singler, Y.W. Zhang, and X. B. Zheng. A superconvergent hybridizable discontinuous Galerkin method for Dirichlet boundary control of elliptic PDEs. *Numer. Math.*, 144:375–411, 2020.
- [37] J. Jiang, N. J. Walkington, and Y. Yue. Stability and convergence of HDG schemes under minimal regularity. *SIAM J. Numer. Anal.*, 63(5):2048–2071, 2025.
- [38] M. Karkulik. A finite element method for elliptic Dirichlet boundary control problems. *Comput. Methods Appl. Math.*, 20(4):827–843, 2020.
- [39] K. Kunisch and B. Vexler. Constrained Dirichlet boundary control in L^2 for a class of evolution equations. *SIAM J. Control Optim.*, 46(5):1726–1753, 2007.
- [40] D. Leykekhman and M. Heinkenschloss. Local error analysis of discontinuous Galerkin methods for advection-dominated elliptic linear-quadratic optimal control problems. *SIAM J. Numer. Anal.*, 50(4):2012–2038, 2012.

- [41] J.-L. Lions. *Optimal Control of Systems Governed by Partial Differential Equations*. Springer, Berlin, 1971.
- [42] M. Mateos. Optimization methods for Dirichlet control problems. *Optimization*, 67:585–617, 2018.
- [43] S. May, R. Rannacher, and B. Vexler. Error analysis for a finite element approximation of elliptic Dirichlet boundary control problems. *SIAM J. Control Optim.*, 51:2585–2611, 2013.
- [44] G. Of, T. X. Phan, and O. Steinbach. Boundary element methods for Dirichlet boundary control problems. *Math. Method Appl. Sci.*, 33:2187–2205, 2010.
- [45] J. Pfefferer and B. Vexler. Numerical analysis for Dirichlet optimal control problems on convex polyhedral domains. *Numer. Math.*, 157:1937–1974, 2025.
- [46] F. Tröltzsch. *Optimal Control of Partial Differential Equations: Theory, Methods and Applications*, volume 112 of *Graduate Studies in Mathematics*. American Mathematical Society, Providence, RI, 2010.
- [47] J. Česenek and M. Feistauer. Theory of the space-time discontinuous Galerkin method for nonstationary parabolic problems with nonlinear convection and diffusion. *SIAM J. Numer. Anal.*, 50(3):1181–1206, 2012.
- [48] B. Vexler and D. Meidner. *Numerical Analysis for Elliptic Optimal Control Problems*, volume 67 of *Springer Series in Computational Mathematics*. Springer Cham, 2025.
- [49] M. Winkler. Error estimates for variational normal derivatives and Dirichlet control problems with energy regularization. *Numer. Math.*, 144:413–445, 2020.
- [50] H. Yücel and P. Benner. Adaptive discontinuous Galerkin methods for state constrained optimal control problems governed by convection diffusion equations. *Comput. Optim. Appl.*, 62:291–321, 2015.
- [51] H. Yücel, M. Heinkenschloss, and B. Karasözen. Distributed optimal control of diffusion-convection-reaction equations using discontinuous Galerkin methods. In *Numerical Mathematics and Advanced Applications 2011*, pages 389–397, Berlin, 2013. Springer.
- [52] Z. Zhou, X. Yu, and N. Yan. The local discontinuous Galerkin approximation of convection-dominated diffusion optimal control problems with control constraints. *Numer. Methods. Partial Differential Equations*, 30(1):339–360, 2014.